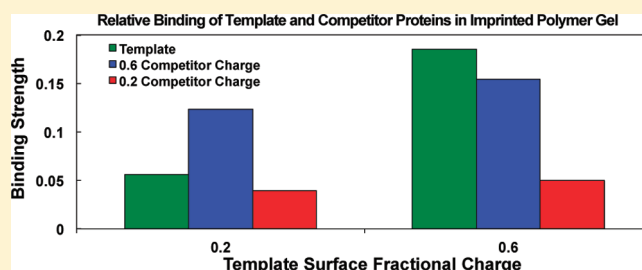


## Simulation of Protein-Imprinted Polymers. 3. Imprinting Selectivity

Liora Levi and Simcha Srebnik\*

Department of Chemical Engineering, Technion — Israel Institute of Technology, Haifa, Israel 32000

**ABSTRACT:** Molecular imprinting has been extensively studied and applied as a simple technique for creating artificial polymer-based recognition gels for a target molecule. Although this technique is effective when targeting small molecules, attempts to extend it to larger templates, such as proteins, have, for the most part, failed to show similar success. Our group has developed a simple simulation model to study protein imprinting. In our previous studies, we investigated the structure of the protein-imprinted pore and imprinting factors of various model proteins. Here, we concentrate on imprinting conditions that affect the separation factor, or the ratio between the interaction energies of the template and a competitor protein. We study the effect of size, charge density, and surface charge distribution of the template protein and calculate the separation factor for various polymerization conditions. Our model captures the known effect of increasing imprinting factor (ratio of binding of the protein in an imprinted polymer to that of a nonimprinted polymer) with increasing surface functionality of the polymer but at the cost of reduced selectivity. Most interestingly, we observe that the surface charge distribution of the protein plays an important role in selectivity of the protein-imprinted polymer, suggesting that some proteins may be better candidates for molecularly imprinted polymers than others.



## 1. INTRODUCTION

The formation of synthetic antibodies using molecular imprinting of biomacromolecules and proteins,<sup>1</sup> if successfully achieved, could potentially offer a generic and cost-effective alternative to existing biological recognition techniques such as monoclonal antibodies that are used in isolation, extraction, biosensors, and other laboratory practices.<sup>2–6</sup> The molecular imprinting procedure is simple and involves the interaction of a template molecule, or analyte, with functional groups via covalent or noncovalent bonds. The complex is then retained through polymerization and cross-linking of monomers to form the imprinted polymer matrix. When the template is removed, a cavity of complementary shape and functionality remains in the polymer, which can, in principle, selectively rebinding the template. A number of alternative imprinting methods have been developed<sup>7</sup> with special interest and methods developed toward imprinting of molecules of biological relevance.

Imprinting of small molecular templates, prominently drugs, has advanced significantly over the years,<sup>7</sup> with applications including clinical analysis, medical diagnostics, environmental monitoring, and drug delivery.<sup>7–13</sup> However, efforts to generate imprints of proteins have, in general, shown limited separation and show relatively high affinity toward competitor proteins.<sup>3,5,14</sup> The difficulties encountered with protein imprinting can be attributed to several factors, such as the use of water as solvent, the presence of multiple weak interactions on the surface of the protein, the relatively flexible conformation of the macromolecule, and the large molecular size of the protein.<sup>2,4,5</sup>

Various protocols have been developed to improve the performance of protein-imprinted polymers (PIPs), including

surface imprinting or the epitope approach,<sup>5,6,11</sup> though the most extensive experimental work on PIPs has focused on three-dimensional imprinting using polyacrylamide gels (PAA) due to their biocompatibility, neutrality, and inert nature that minimizes nonspecific interactions with proteins. Some of the important experimental studies of PAA protein-imprinted gels are referred to in our previous work.<sup>15</sup> We recently carried out lattice Monte Carlo (MC) simulations of the imprinting process using radical polymerization of hydrogels as a simple model for such PIPs.<sup>15,16</sup> Apart from our work, several computational approaches for molecularly imprinted polymers of *small* molecular templates (MIPs) have been introduced during the past decade. As recently reviewed in refs 17–19, most of these studies concentrate on prepolymerization complexation of the templates and functional monomers because a correlation between properties of the prepolymerization solution and final imprinting efficiency has been shown to exist.<sup>20</sup> As discussed by Levi et al.,<sup>21</sup> coarse-grained models of the imprinting process remarkably are able to replicate and give some insight into the origins of experimentally measured trends of MIPs, including the imprinting effect, binding site distributions, and selectivities.

Molecular simulation in this field, however, concentrates on MIPs. Our group was the first to consider coarse-grained modeling of PIPs. We introduced a lattice kinetic gelation model (KGM)<sup>15</sup> of a protein-imprinted polymer gel where, for simplicity, the protein was modeled as a rigid body with randomly

Received: July 20, 2011

Revised: September 22, 2011

Published: October 19, 2011

located functional sites. We carried out a systematic investigation of the structure and porosity of the imprinted gel for various polymerization parameters and studied the structure and functionality of the imprinted pore by diffusion of the model protein inside of the pore immediately following polymerization. One of our prominent results showed that the binding energy of the protein within the imprinted pore is strongly influenced by the overall monomer concentration used in the prepolymerization solution, with minimal recognition of the protein at the percolation limit of protein-sized pores in the gel. PIP selectivity was evaluated by comparing the interaction energy of the protein in the imprinted gel with the energy of a random process (simulated as a statistical configuration of functional monomers and cross-linkers in solution prior to equilibration and gelation). This measure revealed that solution charge concentration has a considerable influence on the extent of recognition in the imprinted gel, achieving a maximum at relatively low charge densities, that is, solutions containing a high concentration of functional monomers result in increased nonspecific interactions, as has also been reported in previous experimental work on protein imprinting<sup>22</sup> as well as simulations of model small molecular templates.<sup>23</sup>

We also compared binding energies and imprinting factors (IFs) of the protein within imprinted and nonimprinted polymers (NIPs) for various compositions and model proteins.<sup>16</sup> In our simulation, the IF is defined as the ratio of average binding energies of the template protein within the imprinted polymer and within a nonimprinted polymer. We focused in this part on two gel types, PIPs and the analogous templated polymers (TPs) formed by imprinting nonfunctional molecules of the same size and shape as the protein in the PIP. We found a significant monotonic increase of IF with monomer concentration,  $\Phi$ . High  $\Phi$  consistently showed up as the most influential factor for imprinting performance, as was seen in previous experimental studies,<sup>24</sup> which, however, must be weighed against the low diffusion rates and protein entrapment that occur in low porosity imprinted gels.<sup>9,11,12</sup> In contrast, TP gels showed an increase in IF with  $\Phi$  only above the percolation limit, and their IF values were always significantly smaller than those of PIP gels, which underlines the essence of imprinting as it shows the significance of combining shape and functionality in order to maximize recognition, where the pore functionality complements the positioning of functional groups on the template protein surface.

In this work, we focus on the separation factor,  $\alpha$ , calculated as the ratio of binding energies of the template protein within the imprinted pore to that of a competitive protein. Focusing on the role of protein size, protein charge density, and charge distribution, we find that IF and  $\alpha$  do not follow the same trends, so that the biomimetic ability of the PIP cannot always be optimized, or in other words, our results strongly suggest that certain proteins might be better candidates for PIPs than others.

## 2. SIMULATION MODEL

Our simulation presents a simple model of protein imprinting via acrylate-based bulk free radical polymerization. Details of the simulation are elaborated in our previous papers.<sup>15,16</sup> Briefly, we carry out lattice simulations, where lattice sites may be occupied by neutral and charged (functional) monomers, cross-linkers, and the rigid cubic model protein. Empty lattice sites correspond to solvent molecules. The protein has a fraction,  $f_p$ , of randomly distributed charged residues that may interact with the charged

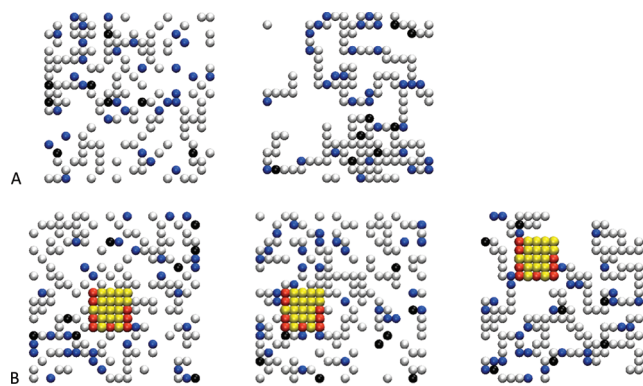


**Figure 1.** Two-dimensional illustration of the lattice simulation model for (a) initialization and polymerization of NIP and (b) initiation, equilibration, and polymerization of PIP. The spheres represent monomers (white), functional monomers (blue), cross-linkers (black), neutral protein residues (yellow), and functional protein residues (red).

monomers in solution. For simplicity, a sufficiently screened solution is considered such that only nearest-neighbor interactions are considered. The charge concentration and fraction in the polymerizing solution and the final gel are defined according to  $\phi_g = N_c/L^3$  and  $f_g = N_c/N$ , respectively, where  $N_c$  represents the number of charged functional monomers and  $N$  is the total number of monomers in the simulation box of dimension  $L$ . Note that  $N$  is the initial number of particles (monomers and cross-linkers) in the simulation. In all simulations, we have considered cases in which the gel fraction is close to unity, and therefore, the difference between  $N$  and the actual number making up the gel is negligible. Simulations were performed on a lattice with  $L = 20$ , which proved sufficiently large.<sup>25</sup>

The simulation model is depicted in Figure 1 in two dimensions for clarity. The simulation begins with random positioning of the protein, cross-linkers, and monomers in the cubic lattice, followed by equilibration (formation of the prepolymerization complex), where noncovalent complexation takes place between the template protein and the functional monomers. The energy of the nearest-neighbor contact between a functional monomer and a charged protein residue is assigned a value of  $-\epsilon$ , while all other nearest-neighbor contacts do not contribute to the energy. We assume screened solution conditions, such that ionic interactions are felt only between nearest neighbors. The dependence of the dielectric constant on the distance between charged species has been indicated by recent experimental and simulation studies of polyelectrolytes.<sup>26</sup> Once equilibrium is reached, KGM is used to simulate gelation,<sup>27–30</sup> beginning with instantaneous initiation where radical “signatures” are randomly distributed among the monomers. Propagation of the polymerization reaction then follows and involves particle moves according to Metropolis acceptance rules and bond formation that takes place upon collision of free radicals with other monomers. Gelation ends either when a single cluster is formed, when all free radicals have terminated, or when the number of clusters does not change for the next  $2 \times 10^5$  iterations, which indicates entrapment of the remaining radicals. At this stage of our study, flexibility of the forming polymer chains is neglected, so that the system is quenched once gelation is completed and the templates are removed, providing a measure of the optimal recognition potential.<sup>20,31,32</sup>

In our previous work, we concentrated on the effect of various parameters on the performance of the gel, focusing on the

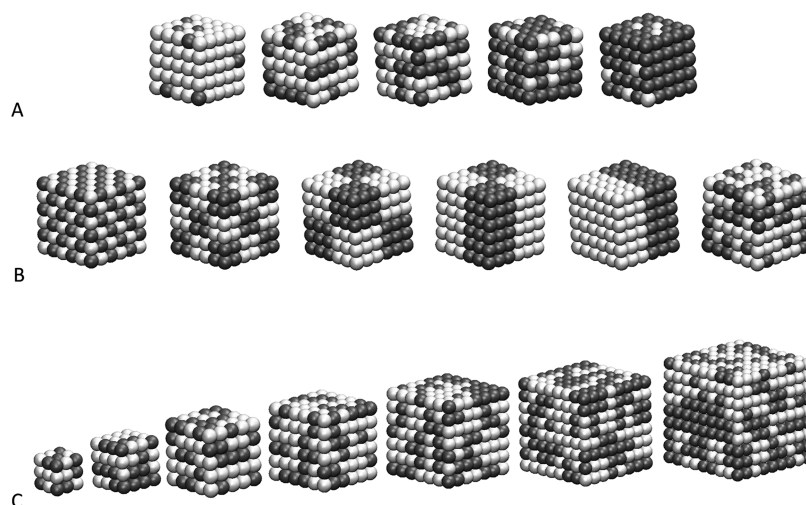


**Figure 2.** Schematic of model proteins with (a) different charge fractions, (b) different charge distributions, and (c) different sizes. Gray represents charged residues and white neutral residues.

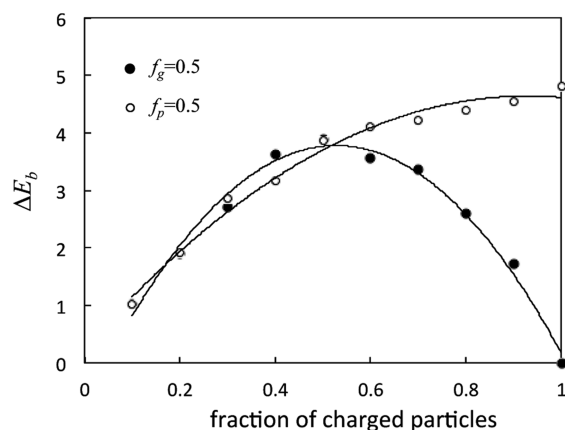


**Figure 3.** Effect of the fraction of charged monomers on the protein (black circles) and within the gel (white circles) on the difference in binding energy between the competitor and the template protein.  $\Phi = 0.4$ .

contribution of site-specific interactions through modeling gelation in the presence of both charged and neutral protein templates. The significantly higher IF seen in PIP over TP gels indicated that our model captures the main features of the imprinting process, where the pore functionality complements the positioning of functional groups on the template protein surface. Here, we address the separation factor of PIP gels for competitor proteins that differ from the template in size, charge densities, or charge distributions, as depicted in Figure 2.

### 3. RESULTS AND DISCUSSION

**Protein versus Gel Functionality.** We use the difference in binding energy between the template protein and competitor,  $\Delta E_b = E_b^c - E_b^t$ , as a measure of specific binding within the imprinted pore. Figure 3 shows  $\Delta E_b$  as a function of the charged residue fraction on the protein surface ( $f_p$ ) and the fraction of charged monomers within the gel ( $f_g$ ). For a fixed  $f_p$ , we find that initially increasing the amount of charged monomers in the gel increases the probability to form specific binding, with the

difference being more pronounced at higher  $f_g$ . That is, highly charged gels more strongly associate with the template. However, energy in itself is clearly not a sufficient measure because, as is well established,<sup>33</sup> a high functional monomer–template ratio results in MIPs with high nonspecific binding due to an excess of charges that are randomly distributed within the polymer matrix. On the other hand,  $\Delta E_b$  changes nonmonotonically with  $f_p$ . The decrease in specificity is due in part to the increase in nonspecific bonds between the protein and template, but more importantly, it is due to the increasing similarity between the template and the competitor protein (at the extreme of  $f_p = 1$ , the template and competitor proteins are identical). Hence, highly charged proteins are not expected to be good candidates for PIPs.

The separation factor,  $\alpha$ , is usually defined as the ratio between the amount of bound template and competitor proteins. Within the simulation framework, one must carry out a grand canonical simulation that involves particle transfer from solution to gel to obtain the relative loadings of the two proteins. However, due to the large size of the template, such transfers are extremely unlikely and could only be carried using biased transfers to predetermined sites of sufficient size within the gel. Because we mainly compare proteins of similar size, the dominant contribution to the partition function is energetic. Hence, we calculate the average interaction energy of our model proteins within such predetermined sites. The interaction energy of the template–monomer complex has been shown to be correlated to the template–polymer binding strength,<sup>34,35</sup> so that we estimate  $\alpha$  as  $\alpha = E_b^t/E_b^c$ , where  $E_b^t$  and  $E_b^c$  are the binding energies of the template and the competitor protein within the PIP, respectively. Figure 4 shows the effect of  $\Phi$  on  $\alpha$  for different charge fractions in the gel ( $f_g$ ) and on the protein ( $f_p$ ). While separation in general tends to improve with increasing  $\Phi$  (higher separation factor), the slope of  $\alpha$  gradually decreases for any given charge fraction, and the decrease is more pronounced with high charge fractions. Moreover, for a highly charged system (circles in Figure 4), selectivity decreases with increasing gel density, although binding of the protein consistently increases with increasing  $\Phi$ .<sup>16</sup> Clearly, charge multiplicity leads to non-specific binding, so that IF is not a sufficient measure in itself for predicting imprinting efficiency. Moreover, Figure 4 clearly indicates that the effect of protein charge is a significantly more



influential factor than the fraction of charged functional groups, with more pronounced selectivity for weakly charged proteins at high  $\Phi$  (compare white symbols).

Figure 5 shows more clearly the effect of charge on  $\alpha$  for different polymer volume fractions, again underlining the more

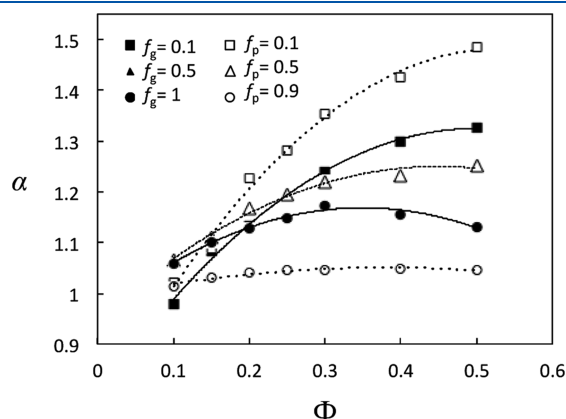


**Figure 4.** Effect of the monomer concentration ( $\Phi$ ) on selectivity ( $\alpha$ ) for various charge fractions of the gel (for  $f_p = 0.5$ ) and of the protein (for  $f_g = 0.5$ ).

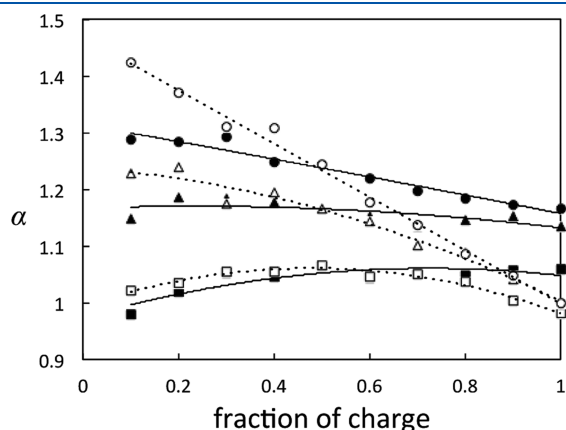


**Figure 5.** Separation factor ( $\alpha$ ) as a function of fraction of charged functional groups within the gel (black symbols, for  $f_p = 0.5$ ) and on the protein surface (white symbols, for  $f_g = 0.5$ ) for various gel densities ( $\Phi = 0.1$  (circles),  $0.2$  (triangles), and  $0.4$  (squares));  $\Phi = 0.2$  marks the percolation limit of protein-penetrable pores).

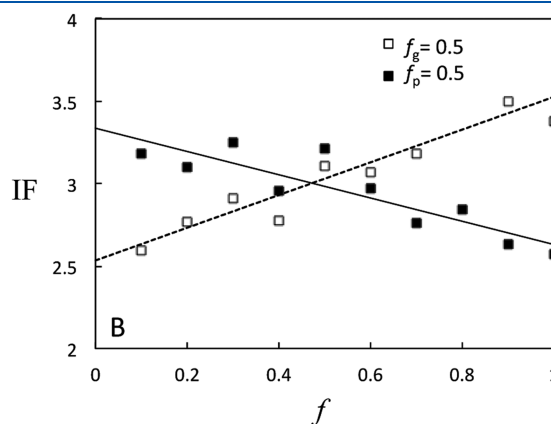
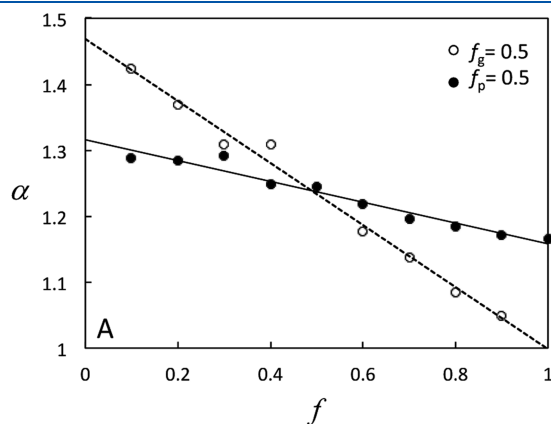


**Figure 6.** Effect of gel charge (black symbols) and protein charge (white symbols) on (a)  $\alpha$  and (b) IF for  $\Phi = 0.4$ .

significant effect of protein charge on selectivity than functional monomer concentration. Furthermore, the percolation threshold ( $\Phi_c = 0.2$ ) distinguished the recognition behavior of the gel (Figure 5, black symbols), that is, separation is improved with increasing charge below  $\Phi_c$  but diminishes with increasing charge above  $\Phi_c$ . However, the behavior of  $f_p$  at different  $\Phi$  is more complex. Above  $\Phi_c$ , highly charged proteins display poorer selectivity (opposite to the effect on IF<sup>16</sup>) because the presence of a large number of charged groups on the protein surface on the one hand decreases the specificity during gelation and on the other hand improves the probability of finding similarly charged areas on the template and on the competitor proteins. Below  $\Phi_c$ , however, a maximum in  $\alpha$  is observed. For the weakly charged proteins, adsorption is favored due to the relatively high functional monomer-to-template ratio. On the other extreme, the highly charged template protein not only presents a relatively indistinguishable surface for imprinting but also lacks a thermodynamic drive for the association of such a large number of monomers in the prepolymerization solution.

We further compare the effects of  $f_p$  and  $f_g$  on  $\alpha$  and IF for  $\Phi = 0.4$  in Figure 6. Figure 6a shows that increasing charge in general, both on the protein and in the gel decrease selectivity, but the effect of  $f_p$  on  $\alpha$  is clearly more significant. In contrast, at this gel density, increasing protein charge improves the IF. Hence, low concentrations of functional monomers in the gel would lead to high imprinting efficiency and higher selectivity, albeit at low efficiencies (low binding).

Imprinting simulations were performed using competitor proteins with different charge fractions than the template protein, shown in Figure 7, for example, for lysozyme ( $f_p \approx 0.2$ ) and cytochrome c ( $f_p \approx 0.6$ ). For the same charge (but different charge distribution) on the competitor and the protein template, Figure 6 shows a slight decrease in  $\alpha$  with increasing charge of the template protein (compare the outermost bars in Figure 7) due to increased nonspecific bonding of the highly charged protein. We predict the highest selectivity for competitor proteins of lower charge than the template protein, and in fact, when a highly charged competitor protein is adsorbed within a gel imprinted with a weakly charged protein,  $\alpha$  takes on values lower than unity. That is, the best selectivity is expected for highly charged template proteins and weakly charged competitors. Reference 36 observed similar results for lys (weakly charged protein) adsorption on the cytochrome c (highly charged protein) imprinted polymer gel. However, whether  $\alpha$  takes on values less than unity for the highly charged cyt on a lys-imprinted gel is

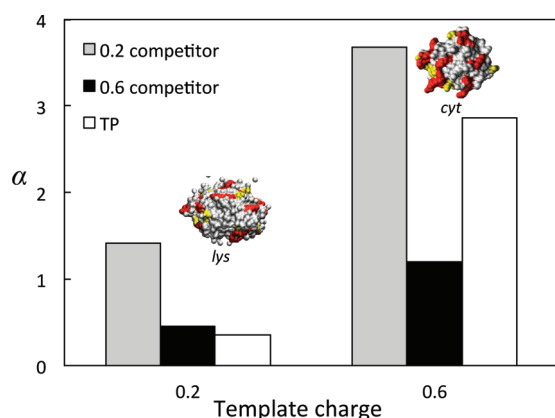


**Figure 7.** Separation factor for template and competitor proteins of different charge ( $\Phi = 0.4$ ). White bars represent the separation factor in the template gel for "template" protein charge 0.2(0.6) and competitor charge 0.6(0.2). Surface charge distributions are shown for lysozyme and cytochrome c as an illustration. Yellow represents negatively charged residues, red represents positively charged residues, and white represents neutral residues.

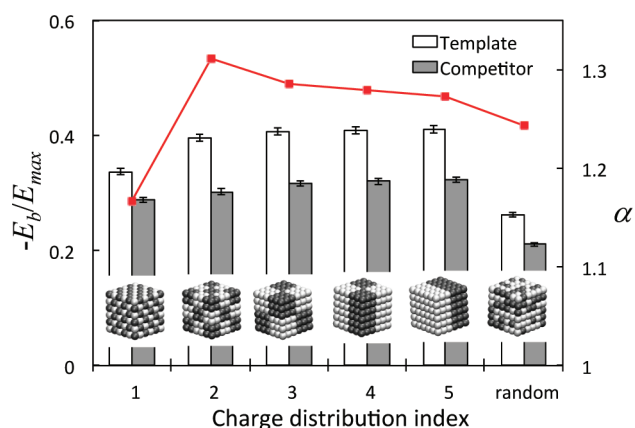


**Figure 8.** Effect of the protein charge distribution on the interaction energy (bars) and separation factor (squares). The competitor protein has the same charge concentration as the template, but with a random distribution of charges.

difficult to assess from the results of ref 36. To isolate the effect of imprinting from that of charge, we compare the "separation factor" between 0.2 and 0.6 charged proteins in TP, shown as the white columns in Figure 7. We clearly see an imprinting effect, though the effect of charge is significant. Presumably, our predicted results underestimate the expected results for real proteins that differ not only in charge density but also in structure, which also significantly contributes to the specificity of the imprinted pores.<sup>16</sup>

**Protein Charge Distribution.** Proteins differ not only in the amount of charged residues on their surface but also in the distribution of charges. The order (or disorder) of charged groups clearly will affect the functionality of the imprinted site and hence should play an important role in recognition of the target protein. Five template charge distributions were considered in addition to the random distribution studied thus far, depicted in Figure 2b, and the results are plotted in Figure 8 for the template proteins with different charged distributions (competitor proteins have the

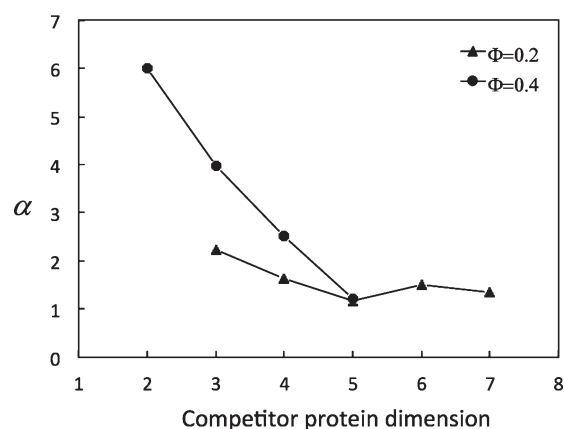


**Figure 9.** Separation factor  $\alpha$  as a function of size of competitor protein for  $\Phi = 0.4$  (circles) and  $0.2$  (triangles);  $f_p = 0.5$ . The size of the template protein is  $d = 5$ .

same charge concentration as the template but with a random distribution of charges). There are four features of Figure 8 that stand out: (1) the imprinting effect is present for all proteins considered ( $\alpha > 1$ ), (2) the randomly distributed template protein shows the poorest binding, (3) the protein with the smallest patches shows the poorest selectivity (lowest  $\alpha$ ), and (4) there is an optimum patch size for best binding and selectivity. The even and uniform charge distribution of protein p1 leads to the formation of uniformly functional pores, which can easily bind other charged proteins and hence shows low specificity. On the other hand, the relatively good binding and high specificity of p2 suggests that proteins with a somewhat patchy charge distribution (such as cyt shown in the inset of Figure 7) may serve as better templates than proteins with either a more uniform or random charge distribution. Very large patches, however, again lead to lower selectivity because the large surfaces of these proteins (p3–p5) present a smooth charged surface that can easily interact with the random patches of the competitor proteins. Such characterization of the protein surface would be revealing and could guide experimentation such as that by Searson and co-workers,<sup>37</sup> who have recently considered the tuning of prepolymerization parameters according to the functional monomer distribution on the protein surface.

**Protein Size.** We carried out simulations for proteins of various sizes but with random distribution of charges, depicted in Figure 2c. For template and competitor proteins of the same size and with random charge distribution, we observed no effect of the separation factor on the size for sizes in the range of  $d = 3$ – $7$ . Results for competitor proteins of different sizes than the template are shown in Figure 9 for template protein size  $d = 5$ . In the porous gel ( $\Phi = 0.2$ ), we observe that  $\alpha$  decreases somewhat with increasing protein size for small competitor proteins but remains relatively constant as we increase the competitor size above that of the template. Therefore, while the difference in protein size significantly affects  $\alpha$  when the competitor protein is small, large proteins that are not too large to enter the imprinted cavity show binding comparable to the template due to an increase in nonspecific interactions as the protein comes into greater contact with pore walls. For the dense gel ( $\Phi = 0.4$ ), only competitor proteins smaller than the template were simulated because the rigid gels considered could not accommodate the larger template. As expected, significant separation is achieved at

high  $\Phi$  when the size of the template protein is considerably different than the competitor protein.

#### 4. CONCLUSIONS

This work presents continuing work on the simulation of protein imprinting. In our previous work, we studied the effect of different simulation parameters on the gel structure, pore functionality, and imprinting factors (IFs) of PIP and templated polymer (TP) gels. In the present paper, we concentrated on the effect of various parameters on the performance of the imprinted polymer, focusing on the separation factor,  $\alpha$ , which measured the binding capacity of the imprinted gel toward its template compared with a competitor protein. We studied the effect of two properties of the gel, the polymer density ( $\Phi$ ) and charge fraction within the gel ( $f_g$ ) on the separation factor, in addition to the size, charge density, and charge distribution of the template protein.

Our results show that  $\alpha$  decreases in highly charged systems due to increased nonspecific binding. Hence, increasing the protein charge impairs PIP selectivity toward the template protein because despite the higher IFs, it does not improve the separation of the gel. On the other hand, there is a minimal charge concentration that is sufficient for recognition, and therefore, for low density gels, high charge fractions are favorable. When using competitors of various charge densities, we found that a highly charged competitor protein has a notable advantage over a poorly charged template. This result points to the conclusion that in cases of similar protein morphology, the imprinting process is not an efficient tool for protein separation. We conclude that proteins with a relatively high concentration of charged surface residues that are distributed in patches may be the best candidates for PIPs. That is, these proteins have distinguishing surface characteristics and can therefore be imprinted. Our current efforts, therefore, concentrate on classifying surface properties of proteins.

#### AUTHOR INFORMATION

##### Corresponding Author

\*E-mail: simchas@technion.ac.il. Tel. +972-4-8293584. Fax +972-4-8295672.

#### ACKNOWLEDGMENT

This research was supported, in part, by the Israel Science Foundation.

#### REFERENCES

- (1) Ge, Y.; Turner, A. P. F. *Trends Biotechnol.* **2008**, *26*, 218.
- (2) Bossi, A.; Bonini, F.; Turner, A. P. F.; Piletsky, S. A. *Biosens. Bioelectron.* **2007**, *22*, 1131.
- (3) Hansen, D. E. *Biomaterials* **2007**, *28*, 4178.
- (4) Turner, N. W.; Jeans, C. W.; Brain, K. R.; Allender, C. J.; Hlady, V.; Britt, D. W. *Biotechnol. Prog.* **2006**, *22*, 1474.
- (5) Zhou, X.; Li, W. Y.; He, X. W.; Chen, L. X.; Zhang, Y. K. *Sep. Purif. Rev.* **2007**, *36*, 257.
- (6) Takeuchi, T.; Hishiya, T. *Org. Biomol. Chem.* **2008**, *6*, 2459.
- (7) Alexander, C.; Andersson, H. S.; Andersson, L. I.; Ansell, R. J.; Kirsch, N.; Nicholls, I. A.; O'Mahony, J.; Whitcombe, M. J. *J. Mol. Recognit.* **2006**, *19*, 106.
- (8) Jiang, X. M.; Jiang, N.; Zhang, H. X.; Liu, M. C. *Anal. Bioanal. Chem.* **2007**, *389*, 355.
- (9) Hilt, J. Z.; Byrne, M. E. *Adv. Drug Delivery Rev.* **2004**, *56*, 1599.
- (10) Alvarez-Lorenzo, C.; Concheiro, A. *J. Chromatogr., B* **2004**, *804*, 231.
- (11) Sellergren, B.; Allender, C. J. *Adv. Drug Delivery Rev.* **2005**, *57*, 1733.
- (12) Duarte, A. R. C.; Casimiro, T.; Aguiar-Ricardo, A.; Simplicio, A. L.; Duarte, C. M. M. *J. Supercrit. Fluids* **2006**, *39*, 102.
- (13) Zhang, H. Q.; Ye, L.; Mosbach, K. *J. Mol. Recognit.* **2006**, *19*, 248.
- (14) Fu, G. Q.; Yu, H.; Zhu, J. *Biomaterials* **2008**, *29*, 2138.
- (15) Levi, L.; Srebnik, S. *J. Phys. Chem. B* **2010**, *114*, 107.
- (16) Levi, L.; Srebnik, S. *J. Phys. Chem. B* **2010**, *114*, 16744.
- (17) Levi, L.; Raim, V.; Srebnik, S. *J. Mol. Recognit.* **2011** In Press.
- (18) Nicholls, I. A.; Andersson, H. S.; Golker, K.; Henschel, H.; Karlsson, B. C. G.; Olsson, G. D.; Rosengren, A. M.; Shoravi, S.; Suriyanarayanan, S.; Wiklander, J. G.; Wikman, S. *Anal. Bioanal. Chem.* **2011**, *400*, 1771.
- (19) Nicholls, I. A.; Andersson, H. S.; Charlton, C.; Henschel, H.; Karlsson, B. C. G.; Karlsson, J. G.; O'Mahony, J.; Rosengren, A. M.; Rosengren, K. J.; Wikman, S. *Biosens. Bioelectron.* **2009**, *25*, 543.
- (20) Idziak, L.; Benrebouh, A.; Deschamps, F. *Anal. Chim. Acta* **2001**, *435*, 137.
- (21) Levi, L.; Raim, V.; Srebnik, S. *J. Mol. Recognit.* To Appear.
- (22) Janiak, D. S.; Kofinas, P. *Anal. Bioanal. Chem.* **2007**, *389*, 399.
- (23) Dourado, E. M. A.; Sarkisov, L. *J. Chem. Phys.* **2009**, *130*, 214701.
- (24) Ou, S. H.; Wu, M. C.; Chou, T. C.; Liu, C. C. *Anal. Chim. Acta* **2004**, *504*, 163.
- (25) Levi, L.; Srebnik, S. *Macromol. Symp.* **2010**, *291–292*, 258.
- (26) Yin, D. W.; Horkay, F.; Douglas, J. F.; de Pablo, J. J. *J. Chem. Phys.* **2008**, *129*, 11.
- (27) Herrmann, H. J.; Landau, D. P.; Stauffer, D. *Phys. Rev. Lett.* **1982**, *49*, 412.
- (28) Bansil, R.; Herrmann, H. J.; Stauffer, D. *Macromolecules* **1984**, *17*, 998.
- (29) Ghiass, M.; Rey, A. D.; Dabir, B. *Polymer* **2002**, *43*, 989.
- (30) Bowman, C. N.; Peppas, N. A. *Chem. Eng. Sci.* **1992**, *47*, 1411.
- (31) Molinelli, A.; O'Mahony, J.; Nolan, K.; Smyth, M. R.; Jakusch, M.; Mizaikoff, B. *Anal. Chem.* **2005**, *77*, 5196.
- (32) Piletsky, S. A.; Karim, K.; Piletska, E. V.; Day, C. J.; Freebairn, K. W.; Legge, C.; Turner, A. P. F. *Analyst* **2001**, *126*, 1826.
- (33) Andersson, H. S.; Nicholls, I. A. *Bioorg. Chem.* **1997**, *25*, 203.
- (34) Wu, L. Q.; Li, Y. Z. *J. Mol. Recognit.* **2004**, *17*, 567.
- (35) Wu, L. Q.; Sun, B. W.; Li, Y. Z.; Chang, W. B. *Analyst* **2003**, *128*, 944.
- (36) Kimhi, O.; Bianco-Peled, H. *Langmuir* **2007**, *23*, 6329.
- (37) Zayats, M.; Kanwar, M.; Ostermeier, M.; Searson, P. C. *Macromolecules* **2011**, *44*, 3966.